SIMS proceedings paper

SURFACE and INTERFACE ANALYSIS

Received: 7 October 2011 Revised: 27 January 2012 Accepted: 1 February 2012 Published online in Wiley Online Library: 28 February 2012

(wileyonlinelibrary.com) DOI 10.1002/sia.4901

Surface characterization of biological nanodomains using NP-ToF-SIMS

F. A. Fernandez-Lima,[a] J. D. DeBord,[a] E. A. Schweikert,[a]* S. Della-Negra,[b] K. A. Kellersberger[c] and M. Smotherman[d]

This paper describes the application of nanoparticle bombardment with time-of-flight secondary ion mass spectrometry (NP-ToF-SIMS) for the analysis of native biological surfaces for the case of sagittal sections of mammalian brain tissue. The use of high energy, single nanoparticle impacts (e.g. 520 keV Au_{400}) permits desorption of intact lipid molecular ions, with enhanced molecular ion yield and reduced fragmentation. When coupled with complementary molecular ion fragmentation and exact mass measurement analysis, high energy nanoparticle probes (e.g. 520 keV Au_{400} NP) provide a powerful tool for the analysis of the lipid components from native brain sections without the need for surface preparation and with ultimate spatial resolution limited to the desorption volume per impact (~10^3 nm^3). Copyright © 2012 John Wiley & Sons, Ltd.

Keywords: NP-ToF-SIMS; MALDI-FT-ICR-MS

Introduction

Over the last decades, a common pursuit has been the generation of signature molecular ions from a surface of interest and their separation and identification. For the case of biological samples, recent technological advances have permitted routine surface interrogation using laser probes [e.g. matrix-assisted laser desorption/ionization (MALDI)], provided that the molecules of interest can be embedded in the crystal lattice of a laser absorbing matrix.[1–4] In MALDI analysis, lateral resolution is restricted to the matrix crystal size and the laser spot (usually tens of microns), with the additional requirement of the pre-selection of a analyte-specific matrix. In a different approach, efforts have focused on the generation of ion probes for enhanced molecular ion emission from native surfaces (e.g. non-modified/untreated surfaces). For instance, the use of nanoparticle projectiles (e.g. Au_{400}, NP- ToF-SIMS) for surface analysis and characterization has shown significant advantages due to the enhanced emission of molecular ions and reduced molecular fragmentation in contrast to atomic and polyatomic projectiles.[5–9] With temporally and spatially discrete impacts, the small desorption volume (~10^3 nm^3) and abundant ionized ejecta make these NP probes promising candidates for surface molecule interrogation.[10,11]

In the present paper, brain sections of an animal model of Parkinsonian dysarthria (e.g. *Tadarida brasiliensis* free-tailed bats) are studied using NP-ToF-SIMS in positive and negative mode. Emphasis is made in the molecular ion emission of lipid components as a function of the projectile size and energy. Because of the chemical complexity of the native brain slices, identification of the most abundant lipid components was performed using complementary MS fragmentation and exact mass measurement analysis (e.g., MALDI Fourier transform ion cyclotron resonance mass spectrometry, MALDI-FT-ICR-MS).

Experimental method

NP-ToF-SIMS and MALDI-FT-ICR-MS

A new, in-house built NP-ToF-SIMS setup was used in this study (see Fig. 1). Briefly, the NP-ToF-SIMS setup comprises an Au-Liquid Metal Ion Source coupled to a 100 kV Pegase Platform, with 120 kV total acceleration voltage and two analysis chambers.[12–14] The primary ion projectiles are mass-selected using a Wien filter and focused into the analysis chamber. All ToF-SIMS experiments were performed under single projectile impacts (e.g. impact rate below 500 Hz of individual projectiles per pulse). Negative mode NP-ToF-SIMS was performed in the analysis chamber 1, where the target voltage is held at −10 kV (total NP acceleration voltage of 130 kV, e.g. 130 keV $Au^+_{1\text{-}9}$ and 520 keV Au^{+4}_{400}), whereas positive mode NP-TOF-SIMS was performed in analysis chamber 2, where the target voltage is held at +10 kV (total NP acceleration voltage of 110 kV, e.g. 110 keV $Au^+_{1\text{-}9}$ and 440 keV Au^{+4}_{400}).

Emitted electrons/protons and negative/positive secondary ions were collected per single projectile impact, respectively. In the negative mode, the emitted electrons were accelerated

* *Correspondence to: E. A. Schweikert, Department of Chemistry, Texas A&M University, College Station, TX 77843–3144, USA. E-mail: schweikert@chem.tamu.edu*

a *Department of Chemistry, Texas A&M University, College Station, TX 77843-3144, USA*

b *Institut de Physique Nucléaire, Orsay, 91406, France*

c *Bruker Daltonics, Inc., Billerica, MA 01821, USA*

d *Department of Biology, Texas A&M University, College Station, TX 77842-3258, USA*

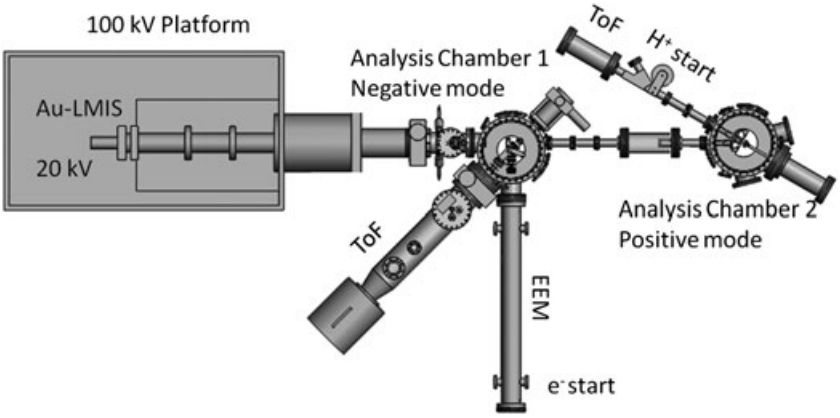

Figure 1. Schematic of the newly built NP-ToF-SIMS analyzer coupled to the 100 kV Pegase Platform. Notice that analysis chambers 1 and 2 are used for negative and positive ion modes, respectively.

from the target and then deflected using a weak magnetic field toward an electron emission microscope and used as a ToF start signal. Secondary ions were accelerated and analyzed using an in-house built ToF analyzer (~1.7 meters long) equipped with a two-stage electrostatic mirror (mass resolution of ~1000–1500). In the positive ion mode, the emitted protons (H^+) were deflected using a magnetic field towards a ToF start detector, whereas secondary ions were accelerated toward a linear ToF analyzer (~1 meter long and mass resolution of ~200–500). It should be noted that positive mode NP-ToF-SIMS analysis was performed as a proof of concept experiment for the NP induced molecular ion emission, not for direct identification of the lipid components considering the low mass resolution of the linear ToF analyzer coupled to analysis chamber 2. In both modes, secondary ion ToF signals were detected using a newly designed, pie-shaped eight-anode detector (up to eight isobaric ions) and were stored on a multi-channel time-to-digital converter. New data acquisition and processing programs Surface Analysis and Mapping of Projectile Impacts (SAMPI) were developed in-house to optimize multiple secondary ion detection.

Lipid assignment of the most abundant peak signals was performed using MALDI ToF/ToF experiments (4700 Proteomic Analyzer; Applied Biosystems Inc., Farmingham, MA) in reflectron ion mode and exact mass measurements using a 12 T solariX MALDI-FT-ICR-MS (Bruker Daltonics, Inc., Billerica, MA). Analysis was performed in both positive and negative ion modes on serial sections. In particular, MALDI-FT-ICR-MS analysis was performed with a lateral pixel resolution of $50 \times 50\,\mu m^2$ and with an average of 500 laser shots per pixel.

Sample preparation

Brain tissue was obtained from captive Mexican free-tail bats *(T. brasiliensis)* at the Texas A&M University colony. Bats were euthanized by anesthetic overdose and the brain quickly removed and frozen in isopentane for 45 s, prior to storage at −80 °C. Before sectioning, brains were allowed to reach a temperature of −20 °C for 30 min in the cryostat chamber (Leica CM1850, Leica Microsystem Nussloch, Germany). The brain was attached to the cryostat specimen disk using ice slush made from distilled water. Brain sagittal sections 12–15 μm thick were cut and placed on ITO-coated glass microscope slides. NP-TOF-SIMS analysis was performed at this stage. For MALDI experiments, in addition to the previous steps, the samples were coated with a solution of 2,5-dihydroxybenzoic acid dissolved in 50% methanol and 0.2% TFA at a concentration of 30 mg/ml. This matrix solution was applied using Bruker ImagePrep™ (Bruker Daltonics, Billerica, MA) which performs multiple cycles of piezoelectric nebulization of the solution followed by periods of incubation and drying to produce a uniform coating across the tissue.

Results and discussion

The secondary ion emission strongly depends on the projectile size and energy. For organic targets, most of the analytical information is extracted from the measurement of analyte-specific fragment ions and/or molecular ions of the species of interest. Previous studies on model organic targets (e.g. single amino acids) have shown that molecular ion emission for the case of polyatomic projectiles ($n = 1$–4) reaches a maximum at ~40 keV per atom; for example, experimental results from Au_3 projectiles on a phenylalanine target ($[M\text{-}H]^-$, $m/z = 164.2$) have shown a maximum desorption yield around ~120 keV.[15] Nevertheless, preliminary results have shown that for the case of larger projectiles (e.g. Au_{400} NPs on a Glycine target, $[M\text{-}H]^-$, $m/z = 74$), the molecular ion emission increases with the projectile energy.[12]

Fig. 2 shows representative ToF-SIMS spectra for 130 keV Au_3, 520 keV Au_{400} NP (negative mode), and 440 keV Au_{400} NP (positive mode) single impacts on the same cerebellum region of native, bat brain sagittal section. ToF-SIMS spectra correspond to ~10^6 impacts (30–40 min acquisition), and the analytical information corresponds to ~ 1% of the field of view ($\sim 100 \times 100\,\mu m^2$) and to the top upper layers (e.g. 10-20 nm for 500 keV Au_{400} NP impacts). Three main features can be observed from the comparison of the secondary ion emission profiles shown in Fig. 2: (i) similar analyte-specific fragment ions, (ii) enhanced molecular ion emission for the case of Au_{400} NP impacts compared with Au_3 impacts (near two orders), and (iii) abundant molecular ion emission of the lipid components for Au_{400} NP impacts (positive and negative

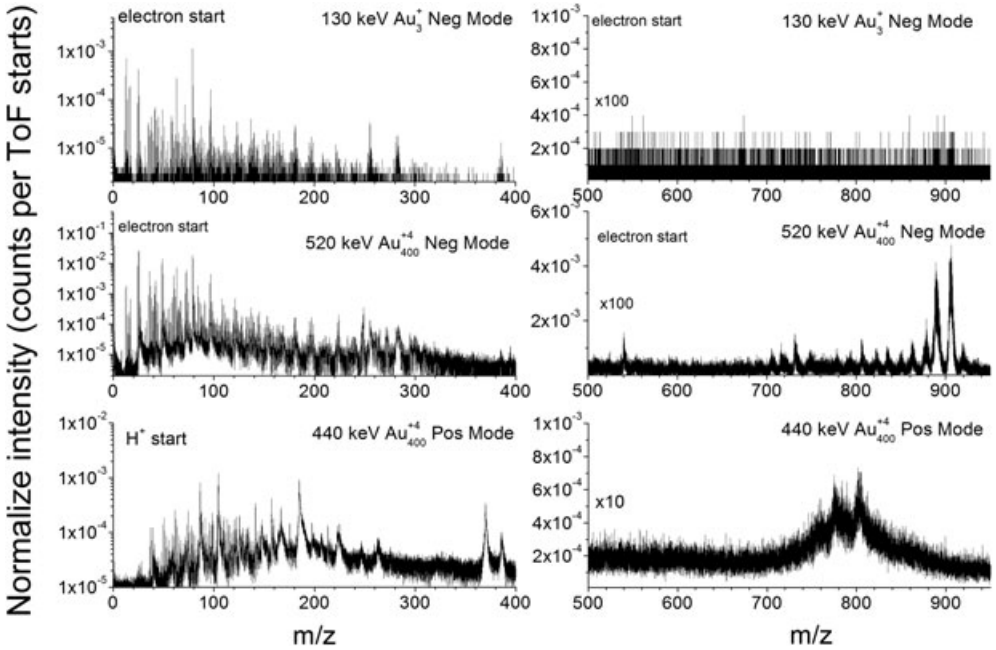

Figure 2. Typical secondary ion spectra obtained from a bat brain sagittal section for 130 keV Au_3, 520 keV Au_{400} NP projectiles (negative mode, reflectron ToF, mass resolution 1000–1500), and 440 keV Au_{400} NP projectiles (positive mode, linear ToF, mass resolution 200–500). Notice the enhanced molecular ion emission for the case of Au_{400} NP projectiles in the $500 < m/z < 950$ region.

mode, yields of ~10^{-2}–10^{-1} molecular ions per impact. Inspection of the low mass region shows abundant emission of $m/z = 26$ (CN^-), 63 (PO_2^-), 79 (PO_3^-), 153 (lipid head group), 184 (lipid head group), 255 (C16:0 palmitic acid), 281 (C18:1 oleic acid), 283 (C18:0 stearic acid), and 386 (cholesterol). In the case of Au_{400} NP impacts, multiple small fragment ions are observed per projectile impact (i.e. more than one ion per impact) compared with ~10^{-2} ion per impact observed with Au_3 projectiles. A significant feature in the case of Au_{400} NP impacts is the backward emission of gold atoms and gold adducts in negative ion mode (e.g. Au^-, $AuCN^-$, and $Au(CN)_2^-$); this is not observed during atomic and polyatomic gold bombardment. We attribute the formation of these gold adducts to the characteristic hydrodynamic penetration of the Au_{400} NP projectiles.[16]

On the other hand, the observation of intact lipid molecular ions permits their unambiguous identification. For example, positive and negative mode analysis using Au_{400} NP ToF-SIMS shows abundant molecular ion emission, with different lipid distributions. We attribute this high lipid abundance as compared with other chemical classes to the fact that lipids account for up to 50% of the dried weight of brain tissue sections. Comparison between positive and negative NP-ToF-SIMS mode shows that molecular ion emission can be directly correlated to the surface concentration and the ionization probability. In particular, two distinct lipid distributions are observed for positive and negative NP-ToF-SIMS modes, which can be attributed to the difference in the charge carriers (lipid head groups) for the different lipid classes. Because of the low mass resolution on the current positive mode NP-ToF-SIMS setup, discussion is limited here to negative ion mode results. To address the large lipid diversity observed in NP-ToF-SIMS, identification of the most abundant lipid species was performed from adjacent sections using MALDI-MS/MS and MALDI-FT-ICR-MS analysis. Fig. 3 presents an expanded view

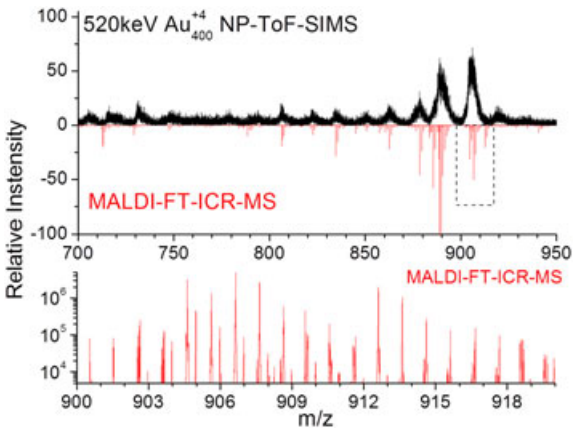

Figure 3. Comparison of the molecular ion emission observed with 520 keV Au_{400} NP projectiles and MALDI-FT-ICR-MS in negative ion mode. Notice the high chemical complexity of the bat brain targets (blow up of the $900 < m/z < 918$ region), i.e. more than one molecular ion per nominal mass.

of the lipid distribution observed with NP-ToF-SIMS and MALDI-FT-ICR-MS (100 μm lateral resolution) for the cerebellum region. Inspection of Fig. 3 shows that a good correspondence is observed between NP-ToF-SIMS and MALDI-FT-ICR-MS lipid distribution. In particular, negative ion mode NP-ToF-SIMS shows high abundance of sulfatides (e.g. ST 18:0, ST: 24:0, ST: 24:1, ST 24:1 OH, and ST 24:0 OH), phosphatidylserines (e.g. PS 40:6) and phosphatidylinositol (e.g. PI 38:4) lipids. The abundant lipid composition and complexity, i.e. multiple lipid molecular ions are observed per nominal mass, is also shown in Fig. 3 for the $m/z = 900$–918 mass range. This result suggests that high resolution separations are necessary for the identification of the most abundant lipid

components; that is, the study of biological targets with high energy NP probes requires the use of high resolution analyzers.

Conclusions

In the present study, we have shown the advantages of using NP-ToF-SIMS for the characterization of native brain sections from mammalian models. Comparison between positive and negative mode NP-ToF-SIMS showed that they provide complementary information on the most abundant lipid species. In particular, a near two-order increase in lipid molecular ion yield is obtained in negative mode NP-ToF-SIMS (e.g. 520 keV Au_{400} NP) compared with traditional ToF-SIMS (e.g. 130 keV Au_3). Comparison of negative mode NP-ToF-SIMS and MALDI-FT-ICR-MS results showed: (i) the chemical complexity of native biological targets, (ii) that NP-ToF-SIMS and MALDI-FT-ICR-MS generate similar lipid distributions (i.e. most abundant lipid components are generated in both cases), and (iii) multiple lipid components are observed per nominal mass. These results also showed that high energy NP probes expand current analytical capabilities for surface interrogation of molecular ions from native biological surfaces. Nevertheless, future efforts will have to focus on increasing NP-ToF-SIMS mass resolution and the incorporation of high resolution separation capabilities (e.g. TIMS-MS[17,18]) for unambigous identification of the desorbed species while keeping high ion transmision and sensitivity.

Acknowledgements

This work was supported by the National Science Foundation (Grant CHE-0750377). F. A. F-L acknowledges the National Institute of Health support (Grant No. 1K99RR030188-01) and a 2010–2011 Bruker Daltonics Inc. fellowship.

References

[1] Y. Sugiura, M. Setou, Selective imaging of positively charged polar and nonpolar lipids by optimizing matrix solution composition Rapid Comm. *Mass Spectrom.* **2009**, *23*, 3269.
[2] T. Jaskolla, B. Fuchs, M. Karas, J. Schiller, The new matrix 4-Chloro-a-cyanocinnamic acid allows the detection of phosphatidylethanolamine chloramines by MALDI-TOF mass spectrometry. *J. Am. Soc. Mass Spectrom.* **2009**, *20*, 867.
[3] K. Teuber, J. Schiller, B. Fuchs, M. Karas, T. W. Jaskolla. Significant sensitivity improvements by matrix optimization: a MALDI-TOF mass spectrometric study of lipids from hen egg yolk, *Chem. Phys. Lipids* **2010**, *163*, 552.
[4] B. Colsch, S. N. Jackson, S. Dutta, A. S. Woods. Brain Gangliosides' molecular microscopy, illustrating their distribution in hippocampal cell layers, *Neuroscience ACS* **2011**, *2*, 213.
[5] C. Lechene, F. Hillion, G. McMahon, D. Benson, A. M. Kleinfold, J. P. Kampf, D. Distel, Y. Luyten, J. Bonventre, D. Hentschel, K. M. Park, S. Ito, M. Schwartz, G. Benichou, and G. Slodzian. High resolution quantitative imaging of mammalian and bacterial cells using stable isotope mass spectrometry, *J. Biol.* **2006**, *5*, 20.1.
[6] M. L. Pacholski, D. M. Cannon, A. G. Ewing, and N. Winograd. Static time-of-flight secondary ion mass spectrometry imaging of freeze-fractured, frozen-hydrated biological membranes Rapid Comm, *Mass Spectrom.* **1998**, *12*, 1232.
[7] C. Guillermier, S. Della Negra, R. D. Rickman, V. Pinnick, E. A. Schweikert. Influence of massive projectile size and energy on secondary ion yields from organic surfaces, *Appl. Surf. Sc.* **2006**, *252*, 6529.
[8] A. Tempez, J. A. Schultz, S. Della-Negra, J. Depauw, D. Jacquet, A. Novikov, Y. Lebeyec, M. Pautrat, M. Caroff, M. Ugarov, H. Bensaoula, M. Gonin, K. Fuhrer, A. Woods. Orthogonal time-of-flight secondary ion mass spectrometric analysis of peptides using large gold clusters as primary ions, *Rapid Comm Mass Spectrom.* **2004**, *18*, 371.
[9] A. Brunelle, S. Della-Negra, C. Deprun, J. Depauw, P. Håkansson, D. Jacquet, Y. le Beyec, M. Pautrat. High desorption--ionization yields of large biomolecules induced by fast C60 projectiles, *Int. J. Mass Spectrom. Ion Processes* **1997**, *164*, 193.
[10] V. T. Pinnick, S. V. Verkhoturov, L. Kaledin, Y. Bisrat, E. A. Schweikert. Molecular identification of individual nano-objects, *Anal. Chem.* **2009**, *81*, 7527.
[11] Z. Li, S. V. Verkhoturov, E. A. Schweikert, Nanovolume analysis with secondary ion mass spectrometry using massive projectiles, *Anal. Chem.* **2006**, *78*, 7410.
[12] S. Della-Negra, J. Arianer, J. Depauw, S. V. Verkhoturov, E. A. Schweikert. The Pegase project, a new solid surface probe: focused massive cluster ion beams, *Surf. Interface Anal.* **2011**, *43*, 66.
[13] F. A. Fernandez-Lima, J. Post, J. D. DeBord, M. J. Eller, S. V. Verkhoturov, S. Della-Negra, A. S. Woods, E. A. Schweikert. Analysis of native biological surfaces using a 100kV massive gold cluster source, *Anal. Chem.* **2011**, *83*, 8448.
[14] F. A. Fernandez-Lima, M. J. Eller, J. D. DeBord, S. V. Verkhoturov, S. Della-Negra, E. A. Schweikert. On the surface mapping using individual cluster impacts, *Nucl. Instr. Meth. Phys. Res. B* **2012**, *273*, 270.
[15] A. Brunelle, S. Della-Negra, J. Depauw, D. Jacquet, Y. Le Beyec, M. Pautrat, K. Baudin, H. H. Andersen. Enhanced secondary-ion emission under gold-cluster bombardment with energies from keV to MeV per atom, *Phys. Rev. A* **2001**, *63*, 022902.
[16] G. J. Hager, C. Guillermier, S. V. Verkhoturov, and E. A. Schweikert. Au-analyte adducts resulting from single massive gold cluster impacts, *Appl. Surf. Sci.* **2006**, *252*, 6558.
[17] F. Fernandez-Lima, D. Kaplan, J. Suetering, and M. Park. Gas-phase separation using a trapped ion mobility spectrometer, *Int. J. Ion Mobility Spectrom.* **2011**, *14*, 93.
[18] F. A. Fernandez-Lima, D. A. Kaplan, M. A. Park. Note: integration of trapped ion mobility spectrometry with mass spectrometry, *Rev. Sci. Instr.* **2011**, *82*, 126106.

